JOURNAL OF MATERIALS SCIENCE 19 (1984) 1406–1419

The effects of amorphous phase separation on crystal nucleation kinetics in $BaO–SiO_2$ glasses

Part 1 *General survey*

A. H. RAMSDEN, P. F. JAMES
Department of Ceramics, Glasses and Polymers, University of Sheffield, Sheffield, UK

The nucleation kinetics of the barium disilicate crystal phase were determined in $BaO–SiO_2$ glasses containing 25.3 to 33.1 mol % BaO at temperatures from 673 to 807°C, using quantitative optical microscopy. The highest nucleation rates were found in the 33.1 mol % BaO glass close to the stoichiometric $BaO \cdot 2SiO_2$ composition, which was just outside the immiscibility region. Much lower rates were observed in the glasses with lower BaO contents including those exhibiting amorphous phase separation. However phase separation had a marked indirect effect on crystal nucleation. Crystal nucleation was strongly dependent on the composition of the baria-rich matrix phase in the phase separated glasses, so that after amorphous phase separation had occurred at a given temperature the crystal nucleation rates of different glasses tended to converge to similar values. There was no evidence from the present results for a significant enhancement of crystal nucleation rates at the interfaces between the amorphous phases. However, nucleation was significantly influenced by certain impurities, particularly alumina, in the glasses. The early stages of crystallization in the glasses were studied by TEM. Immiscibility temperature measurements and results of DTA and X-ray diffraction are also reported.

1. Introduction

Many of the glass compositions used to prepare glass ceramics show amorphous phase separation prior to crystal nucleation and growth. It is well known from the study of phase diagrams that liquid–liquid immiscibility may have a strong influence on the course of crystallization in a system and that liquid unmixing may aid subsequent crystallization by producing a phase with a greater tendency to crystallize than the initial homogeneous glass [1–3]. However, it is clear that amorphous phase separation (often referred to as simply "phase separation") is not essential to produce internal (volume) crystal nucleation in glasses. Thus compositions such as $Li_2O \cdot 2SiO_2$ and $Na_2O \cdot 2CaO \cdot 3SiO_2$ crystallize internally but do not phase separate. Also some systems, for example, compositions in the $Na_2O–SiO_2$ system, phase separate but do not exhibit internal crystallization. Nevertheless, nucleating agents such as TiO_2, P_2O_5 and ZrO_2, which are vital in promoting high internal nucleation rates in certain glasses and in producing fine grain glass ceramics, also increase the tendency towards amorphous phase separation. Consequently there remains some debate on the role of phase separation in the formation of glass ceramics.

Studies of phase separation and crystal nucleation and growth in glasses have been reviewed by various authors [2, 4–7]. Recently James [8] and Craievich *et al.* [9] summarized the current position. Apart from complex multicomponent systems, the effects of phase separation on crystal nucleation even in "simple" two-

0022–2461/84 $03.00 + .12

component systems such as Li_2O–SiO_2 are not clearly understood. In earlier work [10, 11] no direct connection was found between the morphology of phase separation and the nucleation of lithium disilicate crystals, and the number of amorphous droplets was many orders of magnitude higher than the number of crystals, indicating that the droplets were not preferred sites for heterogeneous crystal nucleation. However, later work [12–15] on compositions inside and just outside the immiscibility region showed that enhanced crystal nucleation could be obtained in glasses undergoing amorphous phase separation. Tomozawa [12] attributed an enhanced nucleation rate in a phase separated glass to the presence of diffusion zones (depleted in silica) around the amorphous droplets which acted as favourable sites for crystal nucleation by lowering the effective surface energy. The experimental observations of Tomozawa were largely confirmed by Zanotto and Craievich [15]. It is relevant to note that in Li_2O–SiO_2–P_2O_5 glass ceramics the finest crystal sizes, and by implication the highest nucleation rates, were achieved in glasses which exhibited phase separation [2, 16].

The present work is an attempt to clarify the effects of amorphous phase separation in glass ceramics. We chose the "simple" binary system, BaO–SiO_2, which has similarities to the Li_2O–SiO_2 system and has several ideal features. It has an extensive region of sub-liquidus immiscibility. It also exhibits internal crystal nucleation without deliberate addition of nucleation catalysts, this simplifying interpretation of the results, and the nucleation rates are relatively high but not too high to be conveniently measured.

Part of the BaO–SiO_2 phase diagram [17] including the liquid–liquid immiscibility boundary [18, 19] is shown in Fig. 1. The crystallization of barium disilicate has been studied in the systems BaO–SiO_2 [20–27], Na_2O–BaO–SiO_2 [3] and Li_2O–BaO–SiO_2 [24]. The $BaO \cdot 2SiO_2$ composition melts congruently at 1420° C and a polymorphic phase transformation occurs at 1350° C between the low temperature (orthorhombic) and high temperature (monoclinic) crystalline forms [17, 22, 28, 29]. The relationship between crystal nucleation and growth rates and temperature were determined for a $BaO \cdot 2SiO_2$ glass [24, 27]. The highest internal nucleation rates occurred between 667 and 780° C with a maximum rate at approximately 700° C. James and Rowlands

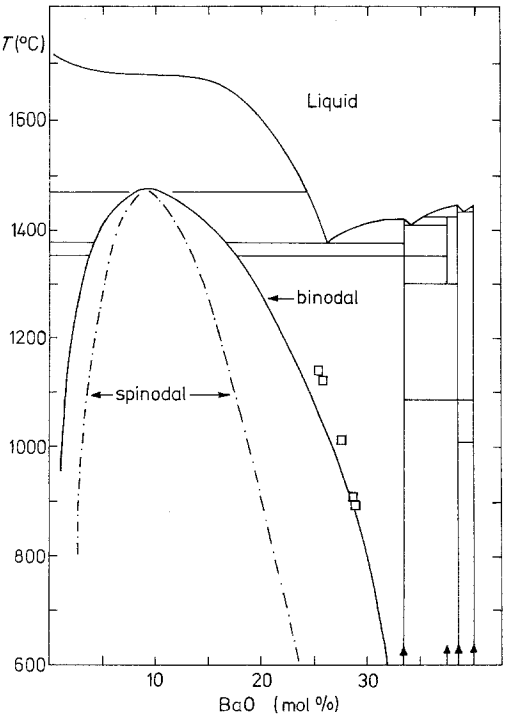

Figure 1 Phase diagram of a section of the BaO–SiO_2 system. Immiscibility boundary (binodal) ——— and spinodal curve —•—•— from [18, 19]. Points □ are from the present work. Liquidus data from [17, 22]. ↑ indicates crystal phases BS_2, B_3S_5, B_5S_8, B_2S_3.

[27] fitted this data to the classical nucleation theory. Using the known heat of fusion and assuming a spherical nucleus they deduced a value of 132 mJ m^{-2} for the crystal–liquid interfacial energy. After nucleation the barium disilicate crystals grow as spherulites, with a complex morphology since both crystallographic forms are involved. However, in the temperature range of internal nucleation the first phase to nucleate appears to be the high (monoclinic) form [3, 24–26].

In the present paper (Part 1) the nucleation kinetics are investigated at various temperatures for a series of BaO–SiO_2 glasses, including some which show amorphous phase separation and others which do not. The method of measuring nucleation kinetics is described, and the possible effects of phase seapration on crystal nucleation are considered. In Part 2 a detailed study of two of the glasses is presented. The crystal nucleation kinetics and development of phase separation are followed simultaneously for isothermal heat treatments at 700° C. Quantitative measurements of the phase separation are obtained by replica electron microscopy. In Part 3 the study is

TABLE I Analysis of high quality commercial sand (wt %)

SiO_2	Al_2O_3	Fe_2O_3	Na_2O	K_2O	CaO	MgO	TiO_2
99.6	0.10	0.01	< 0.05	0.03	0.01	< 0.02	0.03

extended to temperatures above 700° C and the phase separation investigated quantitatively using small angle X-ray scattering (SAXS).

2. Experimental details

2.1. Preparation of glasses and chemical analysis

A series of $BaO–SiO_2$ glasses were melted with compositions in the range 25 to 34 mol % BaO. The batch materials were Analar grade barium carbonate supplied by Fisons (major impurity strontium) and high quality commercial sand (a typical analysis using XRF is given in Table I). After thorough mixing, the batch was sintered in a mullite crucible in an electric furnace at 1300° C for 16 h. The sintered material was ground to pass a 30 mesh sieve and after further mixing was melted in a platinum crucible in a gas-fired furnace at 1550 to 1600° C for 6 h. During melting the glass was stirred continuously by a platinum blade. The glass was then cast, finely crushed and the melting schedule (excluding sintering) was repeated twice. The glasses were finally cast into 1 cm diameter rod on a corrugated steel plate. Some samples were also prepared in the form of thin discs by rapid quenching between steel plates. This was necessary for the glass with the higher silica content to prevent opalescence due to phase separation in cooling.

The above melting procedure was followed to obtain homogeneous glasses. The homogeneity of each glass was tested by examining the uniformity of its crystallization behaviour. Six samples were given a crystal nucleation treatment at 700° C for 1 h, followed by a growth treatment at 840° C for 10 to 30 min and examined in the optical microscope. The number of crystals per unit volume, N_v, was measured in each sample, as described later. A large variation in N_v in the samples (say, 50% or more) indicated a variation in composition. The glass was then considered unsatisfactory and required remelting. However, satisfactory glasses were consistently obtained with the above melting procedure, as shown by only a small variation in N_v (20 to 30% maximum). This procedure was therefore standardized for all the glasses.

Table II lists the glasses and wet chemical analysis results for baria and the impurities alumina and iron. The methods of analysis are described elsewhere [26]. The glass B6, close to the barium disilicate composition, was prepared by James and Rowlands [27] using similar procedures. The iron and alumina impurity levels were generally low. The higher alumina levels in some cases, probably resulted from the sintering stage. Usually the sintered batch could be removed cleanly as a "plug" from the mullite crucible and care was taken after sintering to reject batch immediately in contact with the crucible. Table III gives the compositions of glasses B1, B3 and B6 as determined by electron probe microanalysis (EPMA). The results are in good agreement with the wet chemical analysis. Of particular note, however, is the relatively high level of strontium oxide, the source of this being the $BaCO_3$ starting material.

TABLE II List of $BaO–SiO_2$ glasses with results of wet chemical analysis for BaO and impurities alumina and iron (wt %)

Glass code	Appearance of cast rods/pressed discs	Analysis (wt %)			BaO content (mol %)*
		BaO	Al_2O_3	Fe_2O_3	
B1	opalescent/clear	46.31	0.18	0.06	25.3
B2	clear/clear	49.05	0.02	0.05	27.4
B3	clear/clear	50.33	0.39	0.06	28.5
B4	clear/clear	50.66	0.04	0.03	28.7
B5	clear/clear	52.64	0.22	0.08	30.4
B6	clear/clear	55.78	–	–	33.1
B7	clear/clear	56.80	–	–	34.0
B8	clear/clear	–	–	–	33.0 + 1.0 Al_2O_3

*Calculated.

TABLE III Full analysis (EPMA) of glasses B1, B3 and B6 (wt %) (ND = not detected, 99% confidence limits (±))

Glass code	BaO	SiO_2	SrO	Al_2O_3	Fe_2O_3	Na_2O	K_2O	CaO	TiO_2	ZrO_2
B1	46.03 ± 0.34	52.90 ± 0.28	1.00	0.12	0.03	0.13	0.01	0.03	ND	ND
B3	49.97 ± 0.44	48.95 ± 0.22	1.03	0.36	0.03	0.14	0.02	0.05	ND	ND
B6	55.71 ± 0.57	44.66 ± 0.47	0.38	0.33	0.03	0.17	0.03	ND	ND	ND

2.2. Determination of crystal nucleation kinetics

Glass samples 3 mm thick were given crystal nucleation treatments at temperatures from 673 to 807° C for exactly 1 h in a horizontal tube furnace controlled to within 0.5° C of the heat treatment temperature. The temperature was measured with a Pt/Pt 13% Rh thermocouple placed close to the samples and was monitored continuously. After nucleation the samples were heated at a higher "growth" temperature for a few minutes to grow the nucleated crystals to dimensions observable in the optical microscope. The method is fully discussed elsewhere [8, 30]. A growth temperature of 840° C was found suitable. Also, the nucleation rate was negligible at this temperature. The exact duration of the growth treatment depended on the numbers of crystals and hence on the first stage nucleation treatement, since it was necessary to avoid overlapping of the particles after growth. In practice the required growth time was determined by shining a light through a sample while still in the furnace. When the glass started to change from transparent to translucent the growth treatment was stopped.

It was desirable that the number of nuclei present in the as-prepared glasses (before heat treatment) should be negligible compared with the number after heat treatment. Optical examination of the as-prepared glasses given a single growth treatment showed that this was the case.

After heat treatment the samples were ground flat to remove any surface crystallization, polished with Cerirouge, and very lightly etched in a 0.2' HCl 0.5 HF (vol %) solution. Optical micrographs were then taken on a Leitz reflection microscope at magnifications up to 500 times. The number of crystal spherulites per unit volume, N_V, was determined from the micrographs using the method of Dehoff and Rhines [31] for random plane sections through an ellipsoid. The method is discussed in detail by James [30]. In the present case the crystal particles after double stage heat treatment were close to spherical in shape, thus simplifying the stereological analysis, N_V being given by $2\ N_A Y/\pi$ where N_A is the number of particle intersections per unit area and Y is the mean value of the reciprocals of the measured diameters for all intersections. For each heat treatment measurements were made of the diameters of 300 to 400 particles in a known area of enlarged prints, and N_V was calculated. Typical optical mircrographs are shown in Fig. 2. There were two main sources of error; the random sampling error (purely statistical) and the error due to small compositional variations in the glass. The total effect of these errors was assessed using different samples of the same glass as mentioned

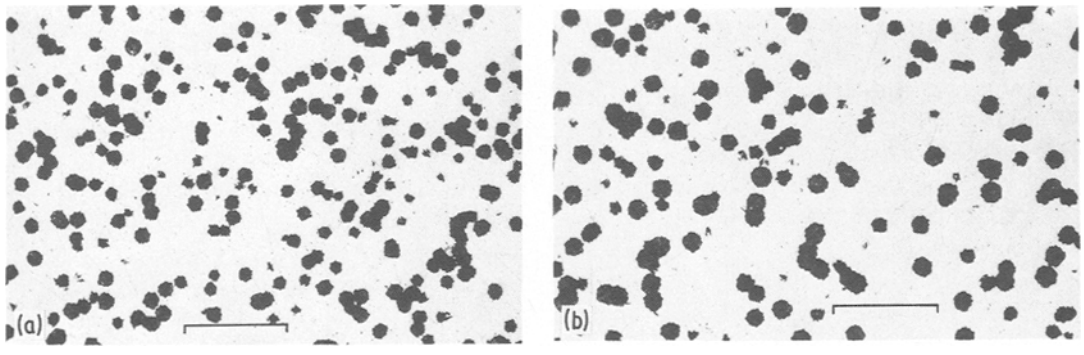

Figure 2 Typical reflection optical micrographs of polished and lightly etched glass sections. Glass B1 nucleated at (a) 721° C for 1 h and (b) 745° C for 1 h, followed by a short growth treatment at 840° C. The bars denote 100 μm.

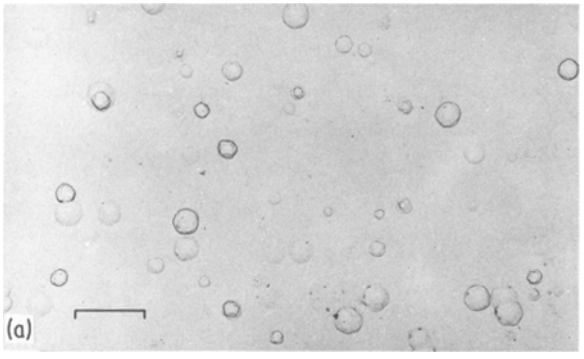

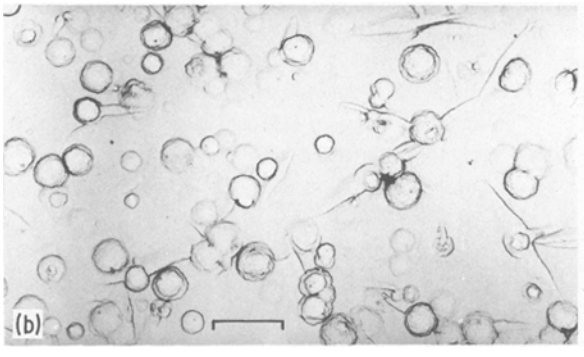

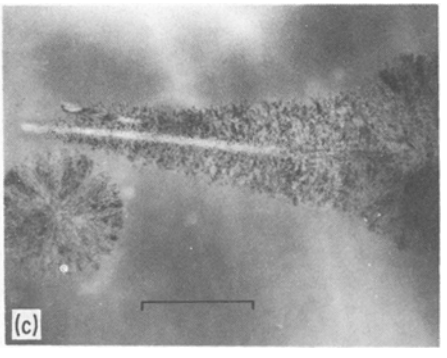

Figure 3 Glass B7 (34 mol% BaO) heat treated at 700° C for 70 h (a) and 116 h (b, c) with no additional heat treatment. Transmission electron micrographs of surface carbon replicas at 75 kV (a, b) and of thin glass section at 100 kV prepared by ion beam machining (c), showing early stages of crystallization in the form of barium disilicate crystalline spheres and needles. The bar denotes 2 μm in (a) and (b); 0.5 μm in (c).

previously. A count of 300 to 400 particles gave N_v with 95% confidence limits of approximately ±15% of N_v. To determine N_v reflection optical microscopy was used in preference to transmission microscopy of thin glass sections. A much larger N_v can be measured by reflection microscopy (upper limit 10^{16} to $10^{17}\,m^{-3}$). For transmission microscopy the specimen thickness must be known and particle overlap is a severe limitation [30].

2.3. Electron microscopy and other techniques used

Transmission electron microscopy (TEM) of both replicas and thin sections was used to study the liquid phase separation morphology and the early stages of crystal growth in the glasses. Carbon–platinum replicas were prepared from polished glass surfaces given a light etch, and examined at 75 and 100 kV in a Hitachi HU11A electron microscope. Thin glass sections were prepared by an Edwards IBMA2 ion beam thinner, and examined at 100 kV in the Hitachi and also in a Philips 301 electron microscope.

Where appropriate, immiscibility temperatures T_m for the glasses were measured. Small chips of glass were heated at a sufficiently high temperature to produce opalescence within a short time. They were then reheated at a series of higher temperatures. The maximum temperature above which the glasses visibly cleared was taken as T_m and could be obtained to ± 5° C. Electron micrographs of the glasses heat treated according to this "clearing" method revealed liquid droplets in the opalescent glass and no evidence of separation in the transparent glass. Differential thermal analysis (DTA) was carried out in a Standata 6-25 apparatus using finely powdered glass samples with powdered alumina as the reference and a heating rate of $10°\,C\,min^{-1}$. The glass transformation temperatures, T_g were found from the endothermic dips on the DTA traces. Crystallized glass samples were examined in a Philips X-ray diffractometer.

3. Results and discussion

3.1. Early stages of crystallization

Samples of glass B7 (close to the barium disilicate composition) were given a *single* stage heat treatment at 700° C for times up to 116 h to produce a large number of very fine crystals suitable for study by electron microscopy (but not optical microscopy).

For heat treatments less than 40 h small spheres (spherulites) composed of numerous fine fibrillar crystallites were the only particles observed on replicas and in thin sections (Fig. 3). Selected area diffraction (Fig. 4) gave patterns of rings and arcs

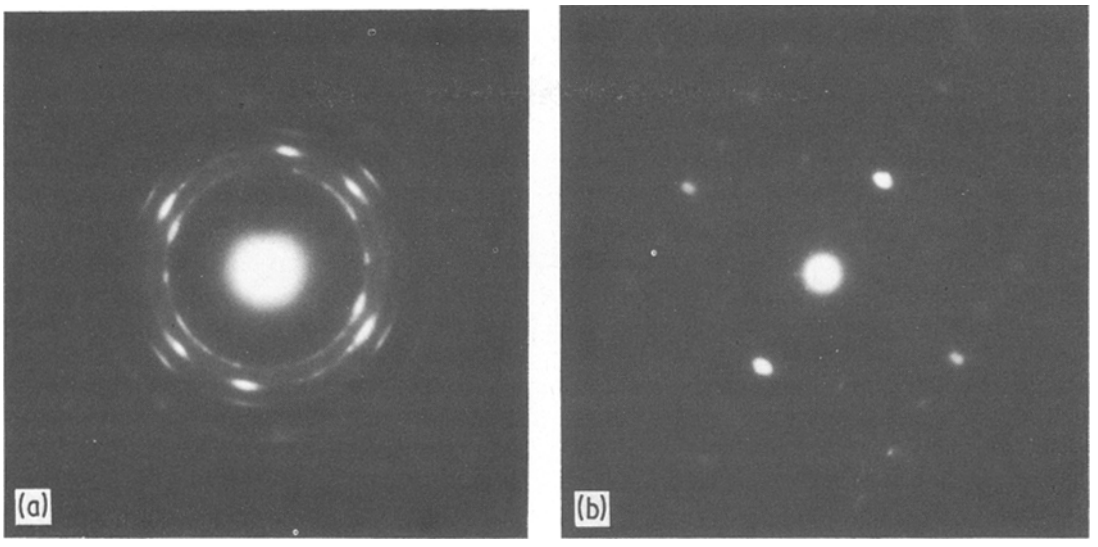

Figure 4 Typical selected area electron diffraction patterns (100 kV) of (a) a small crystalline sphere and of (b) a crystalline needle. Glass B7 heat treated at 700° C for 116 h.

consistent with a radial arrangement of very fine crystallites (10 nm or less in size). The spheres were identified as the high temperature, monoclinic form of barium disilicate ("*h* BS_2") in agreement with other studies [3, 25]. After about 40 h at 700° C additional needle-like growths appeared consisting of a central axial spine with fibrillar side growths. Selected area diffraction patterns of the "needles" contained both sharp discrete spots often as a two-dimensional cross-grating pattern and broader arced spots (Fig. 4). These patterns indicated that the spine was a single orthorhombic crystal of the low form ("*l* BS_2") and the side growths were of the monoclinic form, in agreement with Lewis and Smith [25].

There was clear evidence that the "needles" nucleated and grew from the initial spheres (Fig. 5). The spines grew outwards from the spheres, generally in a radial direction, although in some instances they appeared to grow non-radially. The spines grew more rapidly than the fibrillar side growths producing the characteristic shapes of the needles. In a few cases the nucleation of a second needle on a primary needle was observed. As the time of heat treatment increased the needles contined to nucleate and grow around each central sphere producing larger "composite" spherulites. These larger spherulites were easily observed by optical microscopy, particularly at higher temperatures such as 840° C (the growth temperature used in the determination of N_v, as discussed above).

The dimensions of the largest "needles" and the largest "primary spheres" were measured from the electron micrographs for a series of heat treatment times at 700° C. For the largest needles, both the length of the spine and the length of side growths (half-width) at the base of the needle were measured. Approximate straight line plots were obtained (Fig. 6) indicating constant growth rates. The growth rate of the sphere radius (1.5×10^{-12} m sec^{-1}) was close to the lateral growth rate of the needles (1.4×10^{-12} m sec^{-1}), and both were small compared with the longitudinal growth rate of the needles (9×10^{-12} m sec^{-1}). This confirms the results from electron diffraction that both spheres and the side growth of the needles were composed of the same crystal form (*h* BS_2). Within experimental error the growth line of the spheres (Fig. 6) passes through the origin, demonstrating that the nucleation induction time for the spheres at 700° C is negligible compared with the heat treatment times used. Independent nucleation measurements (see Part 2) support this conclusion. On the other hand, the growth line of the spines (Fig. 6) shows an intercept on the time axis of about 40 h, indicating that there is an induction time before the spines nucleate at the surfaces of the growing spheres. The lateral growth of the needles also gives a similar intercept time showing

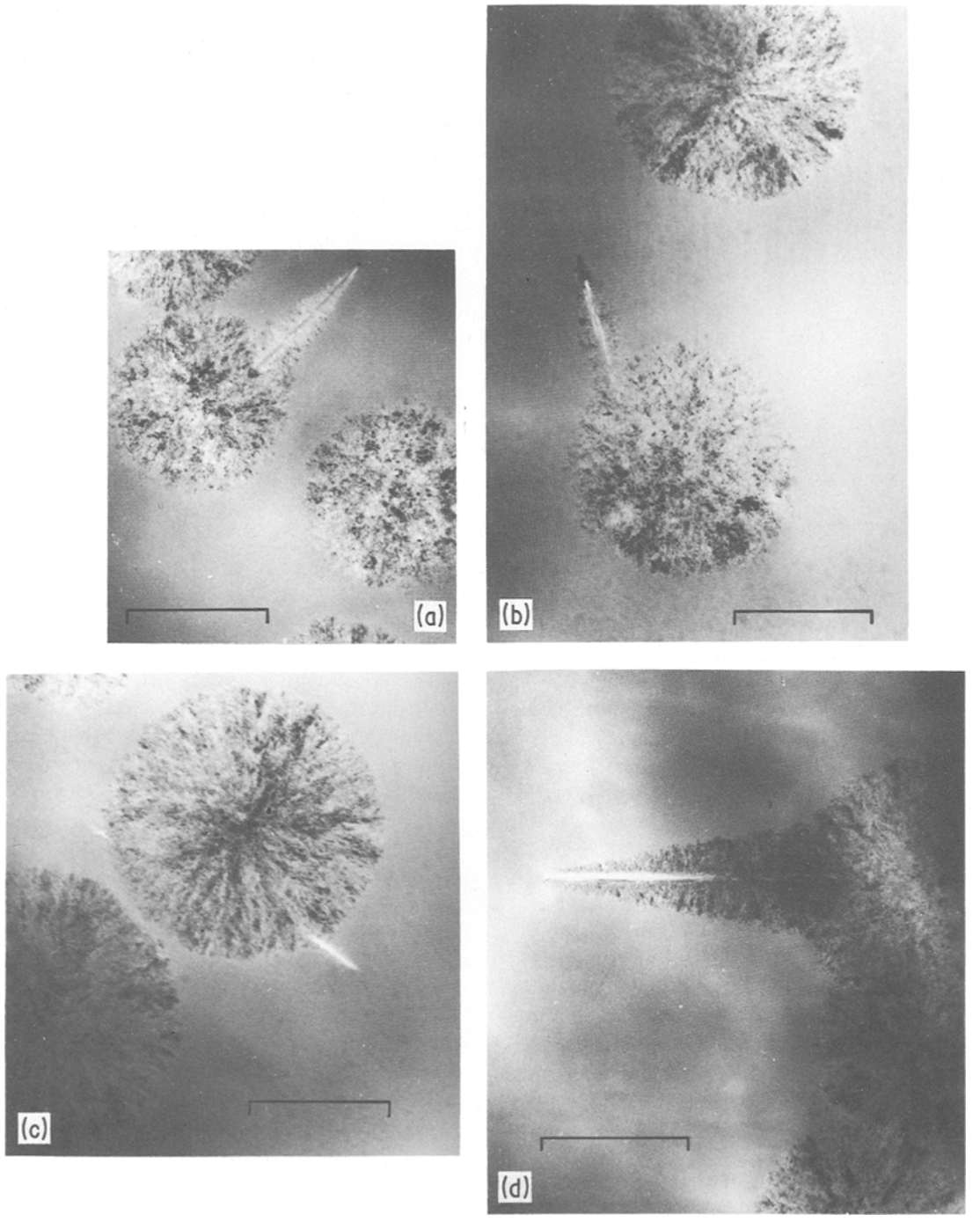

Figure 5 Glass B7 (34 mol % BaO) heat treated at 700° C for (a) 87 h; (b), (c) 96 h; (d) 116 h. TEM micrographs of ion beam thinned glass sections (100 kV) showing crystalline needles of barium disilicate growing from the surfaces of the initial crystalline spheres. The bars denote 0.5 μm.

that the lateral fibrils begin to grow immediately the spine forms.

Growth rates u of spherulites have been determined by optical microscopy at higher temperatures (749 to 868° C) in glass B6 (Table II), close in composition to the present glass (B7) [24, 27]. Extrapolation of these results using a log u against $1/T$ plot (T is temperature in K) shown in

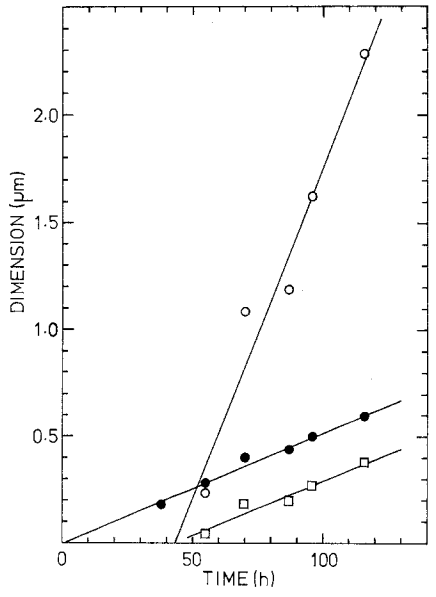

Figure 6 Crystal growth measurements from electron micrographs of thin sections of glass B7 (34 mol% BaO) after heat treatment at 700° C for various times. Radius of largest spheres •; length of largest needles ○; half-width at base of largest needles □.

Fig. 7, gives a growth rate at 700° C of approximately 10^{-11} m sec^{-1}, in agreement with the longitudinal growth rate of the needles obtained in the present work by electron microscopy. This confirms that the radial spherulitic growth measured in [24, 27] can be identified with the longitudinal growth of the needles which nucleate on the central spheres. Furthermore, in previous optical microscopy studies [24, 27] a positive intercept was observed on the time axis of the plots of radius against time. This intercept increased with decrease in temperature, being about 2 h at 749° C [27]. This is again consistent with the change in crystal morphology observed by TEM.

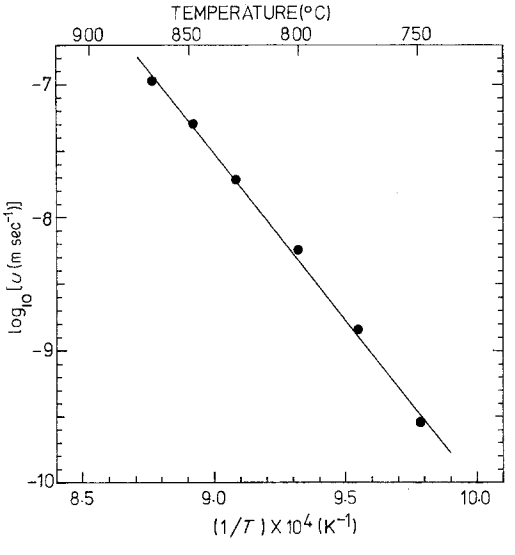

Figure 7 $\text{Log}_{10}u$ against $1/T$ plot, where u is the crystal growth rate in a barium disilicate glass (B6) and T is the temperature (K). Data from [24, 27].

The early stages of crystallization were also studied by TEM in glass B4. Fine-scale phase separation was observed after extended heat treatments at 700° C. However, the crystallization behaviour and crystal morphology were very similar to glass B7, which did not phase separate.

Glasses B4 and B7 were examined by X-ray diffraction. For long heat treatments (>16 h), at high temperatures (>860° C) $l\text{BS}_2$ was identified in both glasses. Traces of cristobalite were also found in B4. At lower temperatures or for shorter heat treatments the X-ray peaks were broad and diffuse and the form of BS_2 could not be identified positively. In this case more information was given by TEM, as described above.

3.2. Liquid–liquid immiscibility

The immiscibility dome calculated from the equation of Haller *et al.* [19], as fitted to the data of Seward *et al.* [18] is shown in Fig. 1. The immiscibility temperatures T_m determined for the present glasses (Fig. 1 and Table IV) are in reasonable agreement with the Haller curve. With the exception of B6, B7 and B8, all the compositions are within the immiscibility dome for most of the crystal nucleation temperatures used.

After the first stage nucleation treatment for 1 hour at temperatures between 650 and 807° C no opalescence in the glasses was observed except for B4 (opalescent at 745, 773° C but clear at 807° C), B3 and B2 (opalescent at 773 and 807° C), and B1 (opalescent at 807° C). However, electron microscopy using replicas revealed

TABLE IV Immiscibility temperatures T_m of BaO–SiO_2 glasses

Glass	Mol% BaO	Experimental T_m (° C)	Calculated T_m (° C) from Haller *et al.* [19]
B1	25.3	1140 (approx.)	1068
B2	27.4	1010	964
B3	28.5	905	901
B4	28.7	890	889
B5	30.4	No immiscibility detected	768

TABLE V Phase separation morphology from EM replicas for glasses B1 to B5 after 1 h at different temperatures (I = interconnected phases, D = droplets, N = no phase separation detected)

Temperature (° C)	B1 (25.3)	B2 (27.4)	B3 (28.5)	B4 (28.7)	B5 (30.4)
807	I	D	D	D	N
773	I	D	D	D	N
745	I	D	D	D	N
721	I	D	D	N	N
709	I	D	N	N	N
As-cast glass	I	N	N	N	N

the presence of fine-scale phase separation in many of the glasses after heat treatment although they were not opalescent. A brief description of the morphology of phase separation for each glass after 1 h heat treatment is given in Table V. Examples of the micrographs will be shown later in Part 2. Where observed the phase separation was always on a fine scale the average droplet diameter varying from 5 to 30 nm approximately.

In general, the greater the silica content of the glass the more rapidly the liquid phase droplets appeared at any given temperature. In B2, for example, droplets were detected after 1 h at 709° C but for B4 there was no evidence of droplets after 1 h at 721° C and below (Table V).

The thermodynamic driving force for nucleation of silica-rich droplets at a given temperature increases as the composition moves from B5 to B1. The composition of B1 is closest to the spinodal boundary (22.4 mol% at 700° C, see Fig. 1) and should have the highest tendency towards phase separation. This was supported by the observations. Thus fine-scale phase separation was observed in B1 even in the as-cast glass.

From Fig. 1 T_m for B5 should be 768° C, in theory. However, no trace of immiscibility could be detected for 1 h treatments below 768° C, before the appearance of internal crystallization, and T_m could not be measured. The driving force for liquid separation was probably so small at temperatures between T_g (about 690° C) and 768° C that liquid unmixing was extremely slow and not observed. Burnett and Douglas [32] also reported a similar temperature gap where immiscibility was not observed in the soda-lime-silica system.

The "DTA T_g" values of glasses B1 to B7 showed no clear trend with composition. The average value was 690° C with a few degrees variation. The main exothermic barium disilicate crystallization peak, the form of which is governed by both crystal nucleation and growth rates, occurred at about 870° C in the glasses with a small variation. A smaller exothermic peak at approximately 1020° C was probably due to recrystallization of the spherulites into lath shaped crystals, as observed elsewhere [24, 27]. A further small exothermic peak was observed in the region 1070 to 1180° C. This was absent for B7 but became increasingly prominent for the higher silica content glasses, and may be due to precipitation of cristobalite (traces of crystobalite were detected by X-ray diffraction in B4 after heat treatment, as shown earlier).

3.3. Nucleation kinetics and the effects of amorphous phase separation

3.3.1. Theoretical considerations

According to classical theory the rate of homogeneous crystal nucleation I at a temperature T for the simplest case of a one component supercooled liquid is given by

$$I = A \exp[-(W^* + \Delta G_D)/kT]$$

where A may be considered essentially constant, W^* is the thermodynamic barrier to nucleation, ΔG_D the free energy of activation for an atom to cross the liquid–solid interface (or "kinetic barrier") and k is Boltzmann's constant. For a spherical nucleus W^* is given by $16\pi\sigma^3 V_m^2/3\Delta G^2$ where σ is the crystal–liquid interfacial free energy per unit area, V_m is the molar volume of the crystallizing phase and ΔG is the Gibbs free energy difference (per mole) between the supercooled liquid and crystal phase.

Liquid–liquid immiscibility might influence crystal nucleation in various ways. The main possibilities have been listed by Uhlmann [33] and James [8], These can be broadly classed as either "composition" mechanisms or "interface" mechanisms.

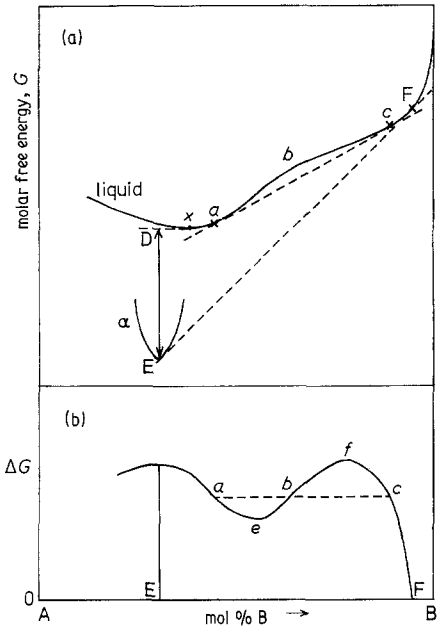

Figure 8 (a) Schematic free energy against composition diagram at a given temperature for a system, similar to $BaO–SiO_2$, exhibiting metastable immiscibility. Metastable equilibrium liquid phase compositions are at a and c, equilibrium compositions for α and liquid are at E and F respectively. (b) Variation of thermodynamic driving force ΔG (distance DE in (a)) with composition for parent non-phase separated glass (solid curve) and for phase separated glass (dotted line).

Local compositional changes as a result of amorphous phase separation may affect W^* (through ΔG or σ) and ΔG_D. Fig. 8 show schematically how ΔG for crystallization depends on whether liquid immiscibility occurs (or not) for a system A–B similar to $BaO–SiO_2$. Suppose the initial composition of the liquid (glass) is at x. If a small region of the equilibrium crystal phase α (e.g., barium disilicate) forms in the liquid it can be shown that, neglecting interfacial effects, the free energy decrease per mole of the crystallizing phase (ΔG) is given graphically by the distance DE [34]. A tangent is drawn to the liquid free energy curve at the initial composition x and DE is the height of this tangent above the free energy curve for the crystal phase, α, at the equilibrium composition. Clearly ΔG will be a maximum for an initial liquid composition at or near the equilibrium composition of α for the case shown in Fig. 8. From Fig. 8 nucleation of phase α, which is sensitive to ΔG, will be enhanced by the occurrence of liquid phase separation for initial compositions between a and b but decreased for initial compositions between b and c. The parent non-phase separated glass shows either a maximum or minimum in ΔG at the spinodal compositions (points of inflexion on the free energy curve). After phase separation (compositions a and c) the glass has a constant ΔG. In the present work we are concerned with compositions between a and e where ΔG will progressively increase until phase separation is complete.

The shift in composition of the liquid phase may also affect the kinetic barrier ΔG_D. ΔG_D may be regarded as the activation free energy for diffusion of the slowest diffusing atomic species in the liquid (possibly oxygen ions [32]). In the present case the diffusion rates will probably be higher in the baria-rich matrix phase than in the parent homogeneous glass. Hence phase separation should result in an increase in crystal nucleation rate I. According to Uhlmann [33] this mechanism is likely to be of paramount importance.

Another factor is the variation of the crystal–liquid interfacial energy with composition. In the $BaO–SiO_2$ system it is likely from theoretical considerations [34] that σ is a minimum when the liquid composition is the same as the stoichiometric barium disilicate crystal phase. This is supported by indirect evidence in the $Li_2O–BaO–SiO_2$ system [24]. Thus I should increase as the glass composition approaches barium disilicate, neglecting the effects of ΔG or ΔG_D. Again, liquid phase separation is expected to produce an increase in crystal nucleation from this source.

There are a number of possible mechanisms associated with the interfaces between the liquid phases that could enhance crystal nucleation:

(a) "Direct" heterogeneous nucleation of crystals at the liquid–liquid interface. However, it is generally considered that such interfaces are unlikely to be strongly preferred sites due to the usually small value of the liquid–liquid interfacial energy compared with the crystal–liquid interfacial energy [8].

(b) Concentration of impurities or surface active agents at the boundaries between the liquid phases causing a locally higher ΔG for crystal nucleation or a locally higher atomic mobility or a lower interfacial energy. A further possibility [35] is the precipitation of a sparingly soluble component at the interface, the precipitates promoting heterogeneous crystal nucleation.

(c) The existence of compositional gradients of the *main* components in the glass around small

liquid droplets causing a locally higher nucleation rate by modifying ΔG, the atomic mobility or σ as in (b). For example, in the $BaO-SiO_2$ system a local depletion of SiO_2 around the droplets undergoing diffusion controlled growth might lead, under certain conditions, to a locally higher ΔG in the depleted zone thereby enhancing the crystal nucleation. As mentioned earlier, Tomozawa [12] has suggested that these compositional gradients might provide site for heterogeneous nucleation, by a mechanism similar to nucleation in a cavity.

3.3.2. Crystal nucleation results

The nucleation results are plotted as $\log_{10} N_v$ (for a constant nucleation time of 1 h) against nucleation temperature in Fig. 9. The values for B6, the nearly stoichiometric barium disilicate glass, were obtained from N_v against time data of Rowlands [24] and James and Rowlands [27] at different temperatures. All the curves show a maximum at between 700 and 720° C. These curves for a constant time t enable the nucleation rates I in the glasses to be compared, particularly at high temperatures above the maximum, where "steady state" conditions apply and I is constant with time at a give temperature. However, non-steady state conditions occur at lower temperatures [8, 30], and N_v/t values underestimate the steady state rates. Here the main purpose is to compare the nucleation (steady state or non-steady state) in the glasses. Also, as Part 2 will show, non-steady state behaviour can be neglected above 700° C. For glasses which phase separate there is an additional complication. Later results (Part 2) will demonstrate that the crystal nucleation rate may vary due to the gradual shift in matrix composition during phase separation.

Let us compare Fig. 9 with the immiscibility results (Tables IV and V). Fig. 9 has two striking features. First, the nearly stoichiometric (barium disilicate) glass, B6, which is just outside the immiscibility gap, has by far the highest N_v values and, hence nucleation rates, at all temperatures. The differences between the curve for B6 and the other curves is from one to three orders of magnitude, depending on temperature. Secondly, the curves for the non-stoichiometric glasses are relatively close together at higher temperatures but more widely spaced at lower temperatures. B5, the glass with the next highest BaO content (30.4 mol%) to B6, had no detectable phase

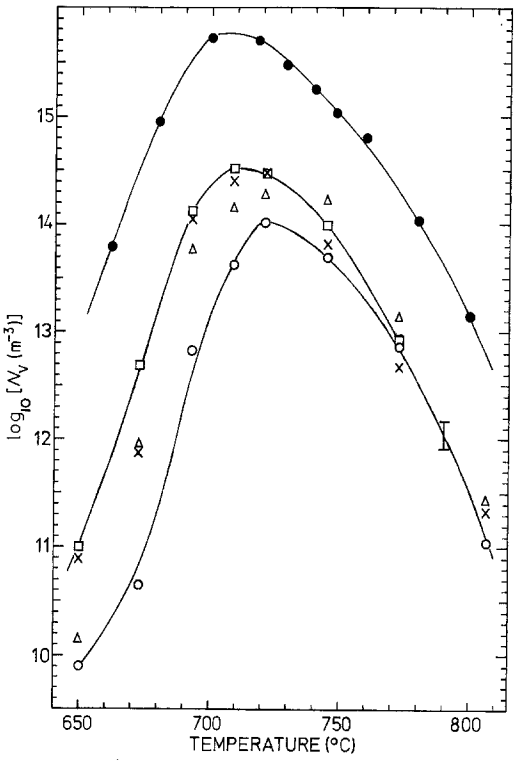

Figure 9 Plots of $\log_{10} N_v(m^{-3})$ against nucleation temperature (° C) for $BaO-SiO_2$ glasses, for a constant time of 1 h at the nucleation temperature. N_v is the number of internally nucleated spherulites of crystalline barium disilicate per unit volume. Glasses, mol% BaO in brackets: B1 (25.3) ○; B2 (27.4) △; B4 (28.7) ×; B5 (30.4) □; B6 (33.1) ●. 95% confidence limits I (approx.).

separation. Apart from B6, B5 showed generally the highest crystal nucleation at 730° C and below and the second highest above 730° C. The glass with the greatest tendency towards phase separation (B1) had generally the lowest crystal nucleation.

These observations appear more consistent with a "composition" mechanism than an "interface" mechanism. TEM indicated that phase separation occurred very slowly at 709° C, and was still in the early stages after 1 h at 709° C. Thus at 709° C and below the glasses would be expected to show differences in crystal nucleation due to their different overall compositions prior to phase separation. The nucleation rates decreased in the order B5, B4, B2, B1, i.e. with decreasing BaO content. This is exactly the order expected for the glasses before phase separation, i.e. in the composition range involved. For a decrease in BaO content the driving force ΔG (Fig. 8) should

decrease, and ΔG_D should increase leading to lower nucleation rates.

At temperatures higher than 709° C phase separation occurred more rapidly. Appreciable phase separation was observed in glasses B1, B2, B3 and B4 (Table V) after 1 h at 745° C. Thus any effects on crystal nucleation rates should become evident at 745° C and above in Fig. 9. These observations are confirmed by recent small angle X-ray scattering data [36], which show that in a 28.3 mol% BaO glass phase separation is essentially complete (the compositions of the phases have attained equilibrium) after 7 h at 743° C and 3 to 4 h at 760° C, whereas in a 27.0 mol% BaO glass it is complete in less than 2.5 h at 743° C. These results will be discussed in Part 3 [37]. According to a "composition" mechanism the nucleation curves for the phase separated glasses should tend to converge at higher temperatures, since at equilibrium the matrix phase at a given temperature has the same composition for all these glasses. This is approximately the case. Subject to experimental scatter, the range of N_v values at low temperatures is much larger than at higher temperatures. For example, at 637° C the range is two orders of magnitude compared with approximately half an order of magnitude at 773° C. The closeness of the curves for the glasses containing 30.4 and 25.3 mol% BaO at 745 and 733° C, compared with their wide separation at lower temperatures is particularly striking.

If it is assumed that crystal nucleation is somehow associated with the interfaces between the amorphous phases, the nucleation rate should be strongly dependent on interfacial area. In general, for the same heat treatment, those of the present glasses well within the immiscibility dome will have a higher volume fraction of silica-rich phase, a more interconnected microstructure and a higher interfacial area per unit volume, as qualitatively observed by electron microscopy. On this basis B1 (25.3 mol% BaO) would nucleate crystals the most readily, followed by the other glasses in increasing BaO content. There would also be a tendency for the curves to separate rather than to converge. These features were not observed experimentally and it is concluded that the interfaces do not have a strong influence on crystal nucleation.

Although agreement with a composition mechanism is good it is not perfect. Thus the N_v values for B2 at 745° C and above appear higher than might be expected relative to the other phase separated glasses even when experimental scatter is taken into account. This is probably due to impurity variations in the glasses. The chief impurities were alumina and strontium oxide. To investigate the effect of Al_2O_3 a glass (B8) of nominal composition $33BaO \cdot 66SiO_2 \cdot 1Al_2O_3$ (mol%) was prepared and nucleated for 1 h at various temperatures. The nucleation was two orders of magnitude lower than in the barium disilicate glass, as shown in Fig. 10. Thus nucleation was sensitive to alumina impurity. Fluctuations in alumina impurity levels (Table II) thus gave small additional changes in N_v. However, these small changes do not affect the main conclusions. Although the effects of strontium oxide impurity were unknown, similar levels were present in all the glasses since the same source of $BaCO_3$ was used. Hence reasonable comparisons of the glasses could be made.

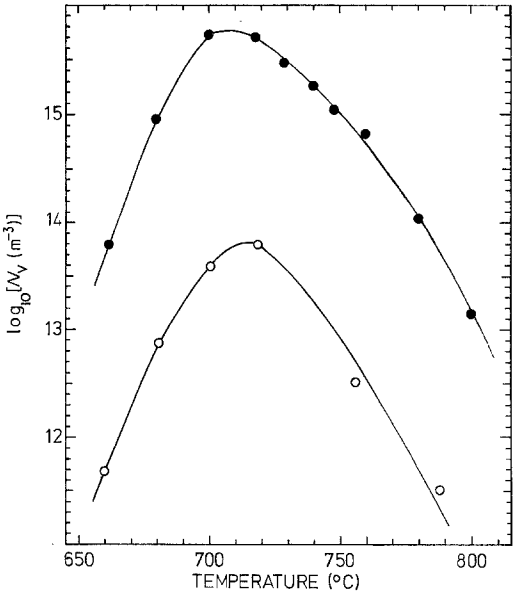

Figure 10 Effect of addition of 1 mol% Al_2O_3 on nucleation in barium disilicate glass. $Log_{10}N_v(m^{-3})$ plotted against nucleation temperature for constant heat treatment of 1 h at each temperature. Glass B6, close to $BaO \cdot 2SiO_2$ in composition (•); Glass B8, nominally (mol%) $33BaO \cdot 66SiO_2 \cdot 1Al_2O_3$ (○).

Strictly, to test the composition mechanism a correction should be made to the nucleation densities N_v for the fact that the values refer to a unit volume of the glass (whether phase separated or not), whereas they should refer to a unit volume of the baria-rich phase in which crystal nucleation occurs. This correction was

carried out [26] at higher temperatures, where phase separation was complete in a short time, by calculating the volume fractions of the baria-rich phase in each glass, using the equation of Haller *et al.* [19] and density data [20]. Since the smallest volume fraction was about 0.8 for glass B1 at 700° C this correction made only a small difference to the values in Fig. 9 and negligible relative changes in the curves.

4. Conclusions

The kinetics of volume nucleation of the barium disilicate crystal phase were determined in BaO–SiO_2 glasses containing 25.3 to 33.1 mol% BaO. The nucleation rates in the glasses exhibiting amorphous phase separation were much less than in the 33.1 mol% BaO glass, close to the disilicate composition, which did not phase separate. However, phase separation had a marked, but indirect, influence on crystal nucleation due to the accompanying shift in composition of the baria-rich phase in which the crystal nucleation occurred. Thus, after heat treatment for 1 h at lower temperatures, where amorphous phase separation was negligible, the crystal nucleation rates were higher the greater the BaO content of the glass, i.e. the closer to the disilicate stoichiometric composition. After heat treatment at higher temperatures where phase separation occurred, the crystal nucleation rates in the phase separated glasses tended to converge, since the matrix compositions in the glasses were closely similar for a given temperature.

The present results indicate that the interfaces between the amorphous phases have, at most, a minor effect on the crystal nucleation kinetics compared with the influence of the phase compositions.

The early stages of nucleation and crystal growth were studied in several of the glasses using TEM. In a glass close to the disilicate composition crystalline spheres (spherulites) of monoclinic BS_2 appeared first during isothermal heat treatment. After an induction time needles nucleated and grew from the surfaces of the initial spherulites. The needles were composed of a central spine of orthorhombic BS_2 and side growths of the monoclinic form, in agreement with previous work [25]. The growth kinetics of needles and spheres as measured by TEM explained the intercepts observed on the time axis in previous studies of the crystal growth kinetics in a $BaO \cdot 2SiO_2$ glass [27]. TEM observations of the crystal morphologies in a phase separated glass (B4) were qualitatively similar to those in the non-phase separated glass B7.

In addition to demonstrating the effects of phase separation and of glass composition on the nucleation kinetics of barium disilicate, the present results showed that nucleation in this system is sensitive to impurities, particularly alumina.

Further experiments are requried to explore the effects of phase separation in more detail and to confirm the ideas proposed in this work. In Part 2 of the present paper experiments will be described in which crystal nucleation is monitored as a function of time in isothermal experiments, that is, while phase separation is taking place.

Acknowledgements

Thanks are due to Mr M. Wilson for carrying out the EPMA work, and to Mr R. Bacon for help with the electron microscopy. AHR was supported by an SERC studentship during the period of this work.

References

1. S. D. STOOKEY, V International Glass Congress, *Glastech. Ber.* **32K** 1959) Paper v/1.
2. P. W. McMILLAN, "Glass Ceramics", 2nd edn. (Academic Press, London 1979).
3. D. G. BURNETT and R. W. DOUGLAS, *Phys. Chem. Glasses* **12** (1971) 117.
4. W. VOGEL, *J. Non-Cryst. Solids* **25** (1977) 170.
5. P. F. JAMES, *J. Mater. Sci.* **10** (1975) 1802.
6. D. R. UHLMANN and A. G. KOLBECK, *Phys. Chem. Glasses* **17** (1976) 146.
7. M. TOMOZAWA, in "Treatise on Materials Science and Technology", Vol. 17, Glass 11, edited by M. Tomozawa and R. H. Doremus (Academic Press, New York, 1979).
8. P. F. JAMES, in "Nucleation and Crystallization in Glasses", Advances in Ceramics, Vol. 4, edited by J. H. Simmons, D. R. Uhlmann and G. H. Beall (The American Ceramic Society, Inc., Colombus, Ohio, 1982) pp. 1–48.
9. A. F. CRAIEVICH, E. D. ZANOTTO and P. F. JAMES, *Bull. Minéral.* **106** (1983) 169.
10. K. NAKAGAWA and T. IZUMITANI, *Phys. Chem. Glasses* **10** (1969) 179.
11. H. HARPER, P. F. JAMES and P. W. McMILLAN, *Discuss. Faraday Soc.* No. 50 (1970) 206.
12. M. TOMOZAWA, *Phys. Chem. Glasses* **13** (1972) 161.
13. K. MATUSITA, T. MAKI and M. TASHIRO, *ibid.* **15** (1974) 106.
14. P. HAUTOJÄRVI, A. VEHANEN, V. KOMPPA and E. PAJANNE, *J. Non-Cryst. Solids* **29** (1978) 365.
15. E. D. ZANOTTO and A. F. CRAIEVICH, *J. Mater.*

Sci. **16** (1981) 973.
16. H. HARPER and P. W. McMILLAN, *Phys. Chem. Glasses* **13** (1972) 97.
17. R. S. ROTH and E. M. LEVIN, *J. Res. Nat. Bur. Standards* **62** (1959) 193.
18. T. P. SEWARD III, D. R. UHLMANN and D. TURNBULL, *J. Amer. Ceram. Soc.* **51** (1968) 278, 634.
19. W. HALLER, D. H. BLACKBURN and J. H. SIMMONS, *ibid.* **57** (1974) 120.
20. J. F. MacDOWELL, *Proc. Brit. Ceram. Soc.* No. 3 (1965) 229.
21. H. TANIGAWA and H. TANAGA, *Osaka Kogyo Gijutsu Shikensho Kiho* **18** (1967) 230.
22. G. OEHLSCHLEGEL, *Glastech. Ber.* **44** (1971) 194.
23. *Idem. J. Amer. Ceram. Soc.* **58** (1975) 148.
24. E. G. ROWLANDS, Ph.D. thesis, University of Sheffield (1976).
25. M. H. LEWIS and G. SMITH, *J. Mater. Sci.* **11** (1976) 2015.
26. A. H. RAMSDEN, Ph.D. thesis, University of Sheffield (1977).
27. P. F. JAMES and E. G. ROWLANDS, in "Phase Transformations", Vol. 2 (The Institution of Metallurgists, Northway House, London, 1979) part III, p. 27.
28. R. M. DOUGLASS, *Amer. Mineral.* **43** (1958) 517.
29. H. KATSCHER, G. BISSERT and F. LIEBAU, *Z. Krist.* **137** (1973) 146.
30. P. F. JAMES, *Phys. Chem. Glasses* **15** (1974) 95.
31. R. T. DEHOFF and F. N. RHINES, "Quantitative Microscopy" (McGraw Hill, New York, 1968).
32. D. G. BURNETT and R. W. DOUGLAS, *Phys. Chem. Glasses* **11** (1970) 125.
33. D. R. UHLMANN, *Discuss. Faraday Soc.* No. 50 (1970) 233.
34. J. W. CHRISTIAN, "The Theory of Transformations in Metals and Alloys" 1st edn (Pergamon Press, Oxford, 1965).
35. S. SCHOLES, *Discuss. Faraday Soc.* No. 50 (1970) 222.
36. E. D. ZANOTTO, A. F. CRAIEVICH and P. F. JAMES, *J. de Phys.* **43** (1982) C9-107.
37. *Idem, J. Mater. Sci.* (to be published).

Received 25 July
and accepted 29 July 1983